



Tube manufacturing and characterization of oxide dispersion strengthened ferritic steels

Shigeharu Ukai^{a,*}, Shunji Mizuta^a, Tunemitsu Yoshitake^a, Takanari Okuda^b,
Masayuki Fujiwara^c, Shigeki Hagi^d, Toshimi Kobayashi^e

^a *O-arai Engineering Center, Japan Nuclear Cycle Development Institute, 4002 Narita, O-arai, Ibaraki 311-1393, Japan*

^b *Kobe Special Tube Co. Ltd., Kobe, Hyogo, Japan*

^c *Kobelco. Ltd., Kobe, Hyogo, Japan*

^d *Sumitomo Metal Industries Ltd., Amagasaki, Hyogo, Japan*

^e *Sumitomo Metal Technology Ltd., Amagasaki, Hyogo, Japan*

Abstract

Oxide dispersion strengthened (ODS) ferritic steels have an advantage in radiation resistance and superior creep rupture strength at elevated temperature due to finely distributed Y_2O_3 particles in the ferritic matrix. Using a basic composition of low activation ferritic steel (Fe–12Cr–2W–0.05C), cladding tube manufacturing by means of pilger mill rolling and subsequent recrystallization heat-treatment was conducted while varying titanium and yttria contents. The recrystallization heat-treatment, to soften the tubes hardened due to cold-rolling and to subsequently improve the degraded mechanical properties, was demonstrated to be effective in the course of tube manufacturing. For a titanium content of 0.3 wt% and yttria of 0.25 wt%, improvement of the creep rupture strength can be attained for the manufactured cladding tubes. The ductility is also adequately maintained. © 2000 Elsevier Science B.V. All rights reserved.

1. Introduction

The oxide dispersion strengthened (ODS) ferritic steels are expected to be more radiation resistant materials than austenitic steels owing to the ferritic microstructure as well as having superior strength resulting from dispersoids at elevated temperature around 973 K. For these characteristic features, ODS ferritic steels are not only prospective cladding material for the long-life core of the liquid metal fast reactors [1,2] but also applicable as low activation fusion reactor materials [3].

Using a basic composition of Fe–Cr–W–Ti– Y_2O_3 , efforts have been made to make cladding tubes of ODS ferritic steels for fast reactors. Grain morphology control by recrystallization has been demonstrated to be necessary in order to soften the materials hardened through cold-rolling and to suppress the strength degradation by grain boundary sliding [4–6]. In this study,

cladding tube manufacturing by means of pilger mill rolling and subsequent recrystallization heat-treatment as well as high temperature mechanical properties for manufactured cladding tubes are characterized as a function of titanium and yttria contents.

2. Experimental procedure

2.1. Manufacturing process

The manufacturing process of the ODS cladding tubes is represented in Fig. 1. The argon gas atomized powder of Fe–0.04C–12.0Cr–0.12Ti (wt%) with a particle size of less than 150 μm was mechanically alloyed with yttrium oxide powder of 20 nm mean diameter. During this treatment, pure titanium powder was also added to adjust the target composition as a function of Y_2O_3 and titanium contents. The 10 kg mass of powder was agitated for 48 h in an argon gas atmosphere at a rotational speed of 220 rpm. The mechanically alloyed powder was then canned, and degassed at a temperature

* Corresponding author. Tel.: +81-29 267 4141; fax: +81-29 267 7130.

E-mail address: uki@oec.jnc.go.jp (S. Ukai).

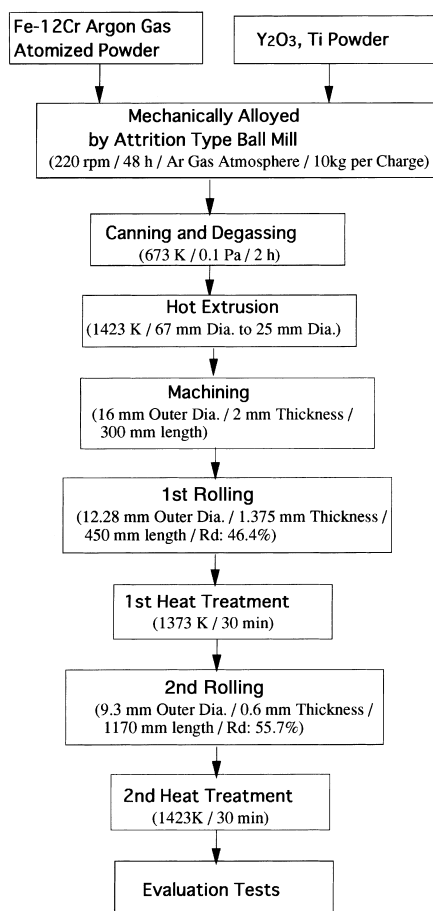


Fig. 1. Cladding tube manufacturing process for F1–F4 specimens.

of 673 K in a 0.1 Pa vacuum for 2 h. Hot-extrusion was conducted to make bars of 25-mm diameter at an elevated temperature of 1427 K. The chemical composition of the consolidated bars is listed in Table 1. The basic composition is Fe–0.06C–12Cr–2W–0.03Ni. Four levels of Y_2O_3 content were selected from 0.08 to 0.24 wt% on the basis of previous experiments, which indicate that

the possible range for recrystallization is less than 0.25 wt%. Titanium is also a dominant element through the formation of Y–Ti complex oxides, which suppress recrystallization. As a result, the titanium content ranged from 0.13 to 0.31 wt%.

Using the consolidated bars, which were machined into the mother tubes with dimension of 16 mm outer diameter and 2 mm thickness, cold-rolling by pilger mill at room temperature was repeated two times resulting in final cladding tubes with dimensions of 9.3 mm outer diameter and 0.6 mm wall thickness. The reduction ratio by pilger mill is approximately 50% for each pass. The heat-treatment was conducted at 1373 K for 30 min after the first rolling, and at 1423 K for 30 min after the second rolling.

2.2. Evaluation tests

Optical microstructure observation and hardness measurements were conducted after each cold-rolling and heat-treatment in order to assess the amount of work hardening or softening and grain morphology changes. For the manufactured cladding tubes, ring tensile tests and pressurized internal creep rupture tests were carried out. The size and inter-particle spacing of the Y_2O_3 dispersoids were evaluated by means of transmission electron microscopy.

3. Results and discussion

3.1. Hardness changes during cladding tube manufacturing

The results of hardness change induced by cold-rolling and heat-treatment in the course of tube manufacturing by pilger-mill are presented in Fig. 2. The hardness of the mother tubes manufactured by the hot extrusion lies between 240 and 380 Hv, increasing with increasing Ti and Y_2O_3 contents. An increase in hardness due to cold-rolling corresponds to around 70 Hv, and the decrease in hardness by heat-treatment is around 80 Hv. These relations of hardness change by

Table 1

Chemical composition of F1–F4 specimens as a function of titanium and yttria contents (wt%)^a

Specimen no.	Chemical composition (wt%)								
	C	Cr	W	Ni	Ti	Y_2O_3 ^b	Ex. O ^c	N	Ar
F1	0.065	11.8	1.92	0.03	0.13	0.08	0.08	0.010	0.005
F2	0.054	11.8	1.94	0.03	0.13	0.13	0.05	0.010	0.004
F3	0.065	11.8	1.93	0.03	0.22	0.22	0.09	0.012	0.005
F4	0.056	11.7	1.92	0.03	0.31	0.24	0.04	0.010	0.004

^a Si = 0.03; Mn = 0.05; P, S = 0.04 (wt%).

^b Estimated from Y content with assumption that Y exists as Y_2O_3 (Y content \times 1.27).

^c Estimated from total oxygen content minus oxygen coupled with Y_2O_3 (total oxygen content – Y content \times 0.27).

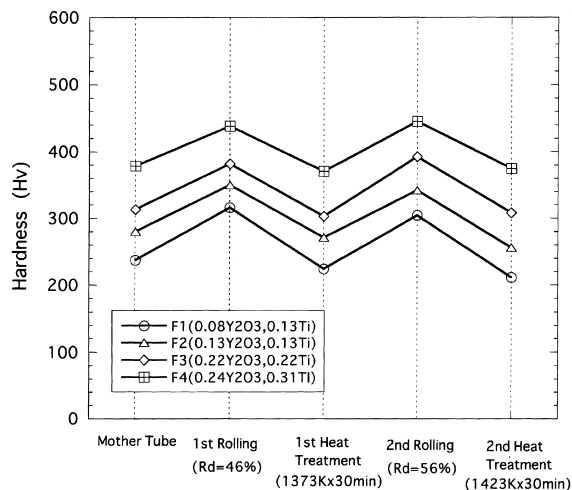


Fig. 2. Hardness history in the course of cladding tube manufacturing for F1–F4 specimens.

cold-rolling and heat-treatment are in agreement with the first and second treatments of tube manufacturing. In particular, four specimens ranging from 0.13Ti–0.08Y₂O₃ (F1 specimen) to 0.31Ti–0.24Y₂O₃ (F4 specimen) exhibit a similar hardness trend.

The optical microstructure change in the course of tube manufacturing for the F4 specimen are shown in Fig. 3, which indicates that recrystallization noticeably occurred both at the first and second heat-treatments. There was no clear difference in the degree of recrystallization for the four specimens. These findings suggest that work hardening and recrystallization do not depend on the titanium and Y₂O₃ contents in the selected range of this experiment. These additive elements result only in an increase in the base line hardness. It is demonstrated from these results that the recrystallized structure is able to be repeatedly realized in at least two heat-treatments, although the recrystallized structure could be restrained at the fourth heat-treatment after complete recrystallization was shown to have occurred in a previous study [6].

3.2. Tensile properties

The mechanical properties of the manufactured ODS cladding tubes were studied. For fuel pin cladding, the circumferential direction is the dominant stress direction. Thus, tensile tests were conducted using the ring specimens prepared from the manufactured cladding tubes. Fig. 4 represents the ultimate tensile strength in the hoop direction at room temperature, 673, 873, 923 and 973 K. With increasing titanium and Y₂O₃ contents, the ultimate tensile strength is linearly increased. An increase in tensile strength due to the addition of both titanium and Y₂O₃ is maintained up to the extended

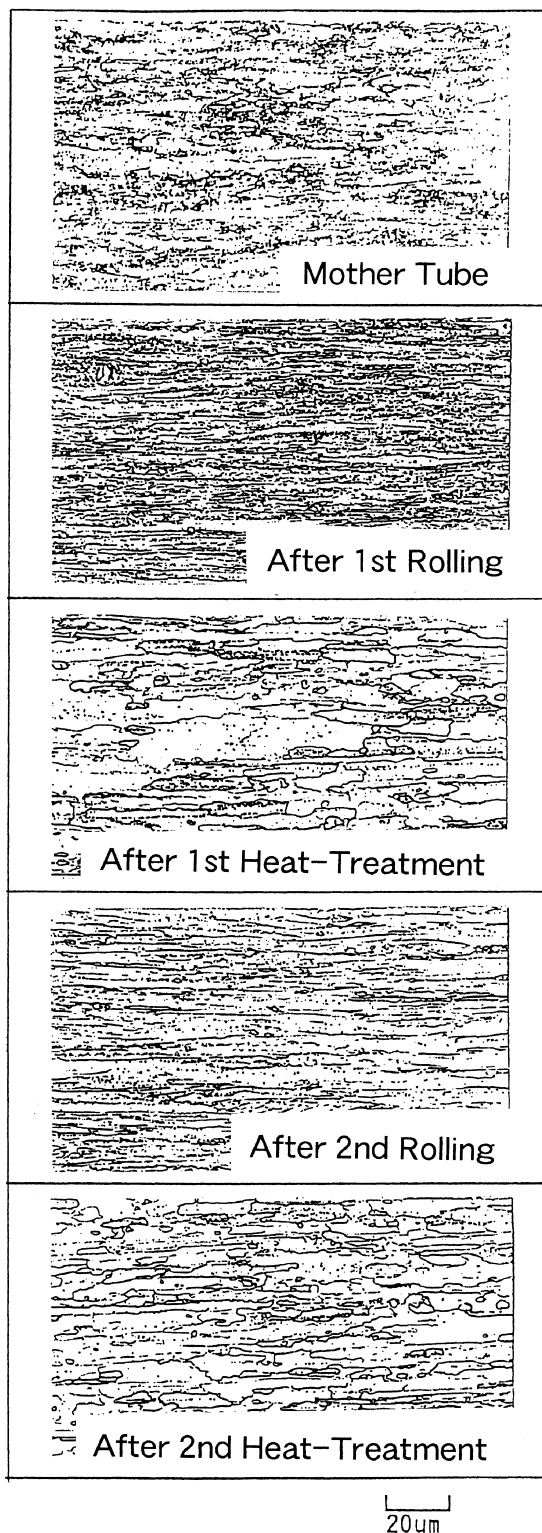


Fig. 3. Optical microstructures of the F4 specimen in the course of cladding tube manufacturing (cold worked and recrystallized structures).

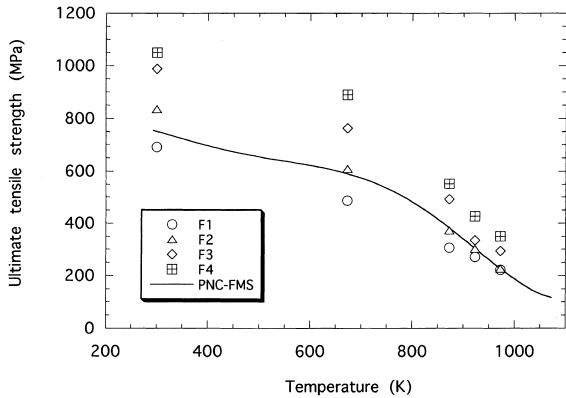


Fig. 4. Ultimate tensile strength in the hoop direction using the ring specimens as a function of test temperature.

temperature of 673 K. However, the difference in tensile strength between the F1 and F4 specimens tends to decrease at temperatures higher than 873 K. The ultimate tensile strength of the ferritic–martensitic stainless steel (PNC–FMS) [7] is also plotted in this figure. The improved strength level in ODS cladding tubes over that of PNC–FMS is also reduced in the higher temperature region.

The uniform elongation is given in Fig. 5. The F4 specimen, showing the highest tensile strength, exhibits lower uniform elongation, but still maintains adequate ductility. In the previous study, nil ductility in the circumferential direction was observed in ring tensile tests for ODS ferritic steels with a bamboo grain structure along the rolling direction [4]. As shown in Fig. 3, the coarse grains induced by recrystallization should suppress the grain-boundary sliding, and thus maintain the ductility over the entire temperature range, even for the

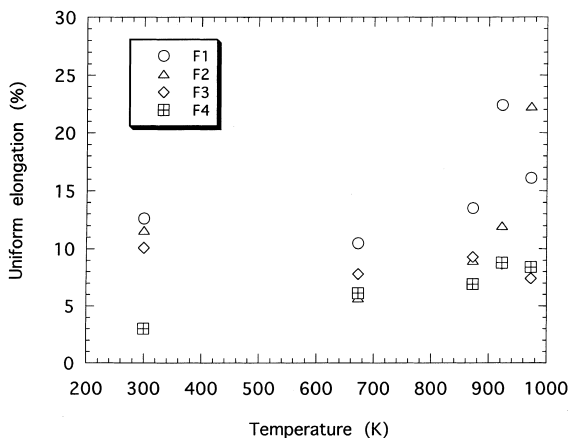


Fig. 5. Uniform elongation in the hoop direction using the ring specimens as a function of test temperature.

F4 specimen. It is also worth noting that ODS ferritic cladding exhibits increasing uniform elongation beyond a temperature of 925 K due to continuing work-hardening, while in commercial ferritic and austenitic steels the uniform elongation decreases in the higher temperature region.

3.3. Creep rupture properties

The creep rupture strengths of F1–F4 specimens at 973 K are exhibited in Fig. 6. The slope of the curve for the F4 specimen seems to be less than those of F1, F2 and F3 specimens, whose creep rupture curves have similar trends. Similar to the tensile properties, the creep rupture strength also tends to increase with increasing Y_2O_3 and Ti contents. For each specimen, the hoop strength levels approaching the short rupture time of 1 h almost coincide with the ultimate tensile strength at 973 K of Fig. 4. In Fig. 6, the creep rupture curve of the PNC–FMS [7] is also shown. Within the rupture time of 200 h, the creep rupture strength of F1–F3 specimens exhibits a similar trend to that of PNC–FMS, while the F4 specimen has a higher creep rupture strength.

Based on transmission electron microscopy of Y_2O_3 dispersoids, a threshold stress for deformation was estimated, according to the Srolovitz’s attractive interaction formula [8] between dispersoids and dislocations. The calculation results in threshold stresses ranging from approximately 80 MPa for the F1 specimen to 170 MPa for the F4 specimen, increasing with increasing Y_2O_3 and titanium contents. This is due to the shortened inter-particle spacing between Y_2O_3 dispersoids. It is also important to note that such estimated threshold stresses for deformation correspond to levels of ap-

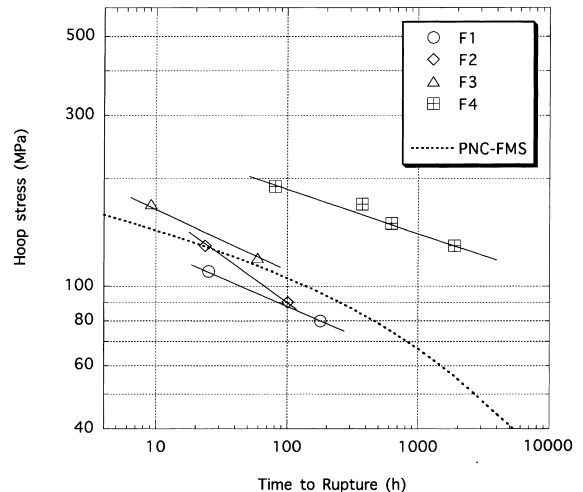


Fig. 6. Internal creep rupture strength in the hoop direction at 973 K.

proximately 0.2% proof stress for all of the specimens. These findings suggest that the time to rupture could extend to longer times at the lower stress level, which may result in the improved creep rupture strength even in F1 specimens in comparison with that of PNC-FMS in Fig. 6. In the case of the F4 specimen, the possibility of attaining the target strength level of around 120 MPa at 973 K for 10 000 h is suggested by extrapolation to longer rupture time.

4. Conclusion

It was demonstrated in these tests that the recrystallized structure is able to be repeatedly realized in the course of tube manufacturing by two cold-rolling passes with a pilger mill and subsequent heat-treatments. For a titanium content of 0.3 wt% and yttria of 0.25 wt%, improvement of the creep rupture strength can be attained for manufactured cladding tubes with a recrystallized structure. The threshold stress for creep deformation was shown to be around the 0.2% proof strength, based on the measurement of dispersoid dis-

tribution; thus the time to rupture could be extended at a lower stress level. The ductility is also adequately maintained.

References

- [1] J.J. Huet, Nucl. Technol. 70 (1985) 215.
- [2] A. Alamo, H. Regle, G. Pons, J.L. Bechade, Mater. Sci. Forum 88–90 (1992) 183.
- [3] D.K. Mukhopadhyay, F.H. Froes, D.S. Gelles, J. Nucl. Mater. 258–263 (1998) 1209.
- [4] S. Ukai, T. Nishida, H. Okada, T. Okuda, M. Fujiwara, K. Asabe, J. Nucl. Sci. Technol. 34 (3) (1997) 256.
- [5] S. Ukai, T. Nishida, T. Okuda, T. Yoshitake, J. Nucl. Mater. 258–263 (1998) 1745.
- [6] S. Ukai, T. Yoshitake, S. Mizuta, Y. Matsudaira, S. Hagi, T. Kobayashi, J. Nucl. Sci. Technol. 36 (8) (1999) 710.
- [7] S. Shikakura, S. Nomura, S. Ukai, I. Seshimo, Y. Kano, Y. Kuwajima, T. Ito, K. Tsutaki, T. Fujita, Nihon-Genshiryoku-Gakkai Shi (J. At. Energy Soc. Japan), 33 (12) (1991) 1157 (in Japanese).
- [8] D.J. Srolovitz, R.A. Petkovic-Luton, M.J. Luton, Philos. Mag. A 48 (5) (1983) 795.